processes

MDPI

Article

Image Analysis Techniques Applied in the Drilling of a Carbon Fibre Reinforced Polymer and Aluminium Multi-Material to Assess the Delamination Damage

Rúben D. F. Sousa Costa [1,2], Marta L. S. Barbosa [2], Filipe G. A. Silva [1,3,4], Tiago E. F. Silva [1], Abílio M. P. de Jesus [1,2], Francisco J. G. Silva [1,5], Luís M. P. Durão [1,5] and João Manuel R. S. Tavares [1,2,*]

1 Laboratório Associado em Energia, Transportes e Aeronáutica, Rua Dr. Roberto Frias 400, 4200-465 Porto, Portugal; rdcosta@inegi.up.pt (R.D.F.S.C.); fgsilva@ispgaya.pt (F.G.A.S.); tesilva@inegi.up.pt (T.E.F.S.); ajesus@fe.up.pt (A.M.P.d.J.); fgs@isep.ipp.pt (F.J.G.S.); lmd@isep.ipp.pt (L.M.P.D.)
2 Departamento de Engenharia Mecânica, Faculdade de Engenharia, Universidade do Porto, Rua Dr. Roberto Frias, 4200-465 Porto, Portugal; up201808522@edu.fe.up.pt
3 Instituto Politécnico Gaya (ISPGaya), Av. dos Descobrimentos 333, 4400-103 Vila Nova de Gaia, Portugal
4 proMetheus, Instituto Politécnico de Viana do Castelo, Rua Escola Industrial e Comercial Nun'Álvares, 4900-347 Viana do Castelo, Portugal
5 CIDEM, ISEP, Politécnico do Porto, Rua Dr. Bernardino de Almeida 431, 4200-072 Porto, Portugal
* Correspondence: tavares@fe.up.pt

Abstract: Due to the high abrasiveness and anisotropic nature of composites, along with the need to machine different materials at the same time, drilling multi-materials is a difficult task, and usually results in material damage, such as uncut fibres and delamination, hindering hole functionality and reliability. Image processing and analysis algorithms can be developed to effectively assess such damage, allowing for the calculation of delamination factors essential to the quality control of hole inspection in composite materials. In this study, a digital image processing and analysis algorithm was developed in Python to perform the delamination evaluation of drilled holes on a carbon fibre reinforced polymer (CFRP) and aluminium (Al) multi-material. This algorithm was designed to overcome several limitations often found in other algorithms developed with similar purposes, which frequently lead to user mistakes and incorrect results. The new algorithm is easy to use and, without requiring manual pre-editing of the input images, is fully automatic, provides more complete and reliable results (such as the delamination factor), and is a free-of-charge software. For example, the delamination factors of two drilled holes were calculated using the new algorithm and one previously developed in Matlab. Using the previous Matlab algorithm, the delamination factors of the two holes were 1.380 and 2.563, respectively, and using the new Python algorithm, the results were equal to 3.957 and 3.383, respectively. The Python results were more trustworthy, as the first hole had a higher delamination area, so its factor should be higher than that of the second one.

Keywords: image processing; image analysis; Python; delamination evaluation; multi-material

check for updates

Citation: Sousa Costa, R.D.F.; Barbosa, M.L.S.; Silva, F.G.A.; Silva, T.E.F.; de Jesus, A.M.P.; Silva, F.J.G.; Durão, L.M.P.; Tavares, J.M.R.S. Image Analysis Techniques Applied in the Drilling of a Carbon Fibre Reinforced Polymer and Aluminium Multi-Material to Assess the Delamination Damage. *Processes* **2024**, *12*, 1258. https://doi.org/10.3390/pr12061258

Academic Editors: Jiaqiang E, Sheng Du, Xiongbo Wan, Zixin Huang and Li Jin

Received: 11 April 2024
Revised: 5 June 2024
Accepted: 11 June 2024
Published: 19 June 2024

Copyright: © 2024 by the authors. Licensee MDPI, Basel, Switzerland. This article is an open access article distributed under the terms and conditions of the Creative Commons Attribution (CC BY) license (https://creativecommons.org/licenses/by/4.0/).

1. Introduction

Image processing and analysis techniques are based on mathematical functions to achieve the intended outcomes for the desired task [1]. Nowadays, many of the advanced engineering developing software tools, such as Matlab (MathWorks, Natick, MA, USA), version 2019 B, or Python (Python Software Foundation, Wilmington, DE, USA), version 5.1.5., already include many of these functions, and the algorithms developed almost only depend on the correct combination of these available functions. Four primary focus areas are usually considered in image processing and analysis: image improvement or enhancement, image restoration, image compression, and image analysis. These focus areas are typically associated with artificial intelligence and are usually designated as computer vision [2]. The first and last areas are the most important in multi-material

drilling processes. In the image improvement or enhancement process, the characteristics of the input image are improved, for example, by accentuating the contrast and reducing the noise. On the other hand, image analysis aims to interpret a given image by measuring or classifying its properties. These techniques can be applied in various fields, such as engineering, science, and healthcare [3].

Usually, the first step in image processing is to convert the input colour image into a grayscale image to simplify the following steps. Afterward, a noise-smoothing technique may be applied to remove unwanted elements in the image surrounding the object(s) of interest, which can be achieved using, for example, a bilateral filter [4] or low-pass filter [5]. Another helpful technique to improve the input image's quality is contrast stretching [6], which increases the contrast between the darkest and brightest regions in the image while preserving the relative differences among the intermediate values. The intensity of the pixels of the object of interest can also be enhanced using sharpening or histogram equalization techniques [7] by modifying the image's intensity distribution based on its histogram or using a high-pass filter.

Another essential function in image processing is the erosion operation, commonly used to erode the boundaries of the object of interest in an image. It can be used, for example, to remove noise, to isolate individual elements, or to reduce the object's size. In the same area, the dilation operation is often used to expand the object's boundaries in a binary image. It can also be used to fill gaps, to connect broken objects, or to increase the object's size. Both have an "iterations" parameter, specifying how often the techniques are applied to the image and how they can be increased to intensify their result [8].

In many applications, after image pre-processing, it becomes necessary to apply the thresholding technique [9], which is the simplest method for performing image segmentation. This technique turns the image into a binary form so that a specific region of interest (ROI) of the image can be emphasised and its subregions can be uniformised. Some other important techniques usually used for this task include the Hough transform technique [10], to detect geometric shapes in images, such as circles; the snake algorithm [11], to find the contour that best approximates the border of an object; and the level set model for image segmentation [12], which implements a geometric active segmentation contour model. From a boundary detection perspective, the Canny, Prewitt, Roberts, and Sobel edge detectors [13,14] are some of the most used operators that perform contour detection in the image under study, using an approximation of its intensity gradient through finite differences. For image analysis, the region-growing algorithm [15] is commonly used to segment image regions by growing a region from a seed point, and then measurements can be obtained from a particular region, allowing for further analyses.

Due to the many possibilities that the usual image processing and analysis techniques offer in solving real-world problems, different applications exist to put them into practice. These range from the automatic evaluation of metallographic microstructure phases [16] and surface characterisations [17] to damage detection in parts resulting from mechanical tests [18] or manufacturing processes in engineering. In the scope of drilling composites and multi-materials, mainly by a combination of composite and metal, several damages usually arise, such as burrs and fibre delamination. This happens mainly due to composite materials' anisotropic nature, making it harder to perform a clean cut. This property, along with the high abrasiveness of the composite fibres and the drill's need to cut through different materials simultaneously, causes severe tool wear, leading to an imperfect surface on the hole's border [19]. This kind of damage may sometimes go unnoticed in high batch production, which could have catastrophic consequences, especially for this process' most frequent applications, the aeronautical and automotive industries [20].

To quantify the hole delamination, some criteria have been proposed in the literature relating the key properties of the damaged regions and those of the original hole. These can comprise just the diameter (F_d), introduced by Chen et al. [21] in 1997, or just the area (F_a), presented for the first time by Mohan et al. [22] in 2007. Later, in the same year, Davim et al. [23] suggested an improved version of the delamination measurement, the

adjusted delamination factor (F_{da}), which is considered a better approximation of reality by combining the diameter and the area at the same time. This can be expressed as:

$$F_d = \frac{D_{max}}{D_{nom}}, \tag{1}$$

$$F_a = \frac{A_d}{A_{nom}}, \tag{2}$$

$$F_{da} = F_d + \frac{A_d}{(A_{max} - A_{nom})}\left(F_d^2 - F_d\right), \tag{3}$$

where D_{nom} and A_{nom} correspond to the nominal hole's diameter and area (in mm and mm^2, respectively), D_{max} and A_{max} to the maximum delamination diameter and area considering the maximum diameter (in mm and mm^2, respectively), and A_d to the actual delamination area (in mm^2) (Figure 1). If the damage around the hole is circular and has a low amplitude, it is not completely considered in the F_d approach, and the same happens for the F_a if there is just a thin crack or a damaged peak but without a great area. That is why the adjusted delamination factor, F_{da}, provides a more complete and more reliable result.

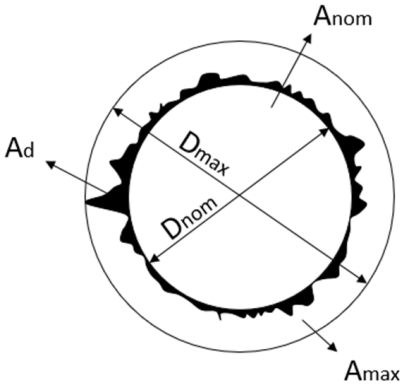

Figure 1. Diameters and areas used to calculate the delamination factors F_d, F_a and F_{da}.

Several studies assess delamination damage in composite materials using image processing and analysis techniques to identify if the non-conformities are within the acceptable limits imposed by the industry quality patterns. Durão et al. [24] used damage assessment image-based methods through computational processing of data extracted from radiographic images and compared them with mechanical test results, bearing and delamination assessment tests, and analytical models, obtaining valuable information regarding the delamination extension and mechanical strength of the drilled parts. In more recent studies, Durão et al. [25] and Devesa et al. [26] used similar methods to calculate the fractal dimension of the damaged region's boundary. Geier et al. [27] predicted drilling-induced burr occurrence in CFRP composites using image processing and analysis by studying the fibre orientation in CFRP sections and their local properties, achieving an accuracy of 64–97% compared to real drilling experiments. Alejandro et al. [28] also autonomously inspected drilled holes in CFRP panels using image processing and analysis techniques to determine the geometric errors and delamination factors for several holes and compared them with experimental results. Despite most delamination assessment approaches through image processing and analysis techniques being applied in just plain composites, machined multi-material processing has been gaining relevance in recent years, even if only a few studies exist on this topic. Isbilir and Ghassemieh [29] studied the hole's quality and respective delamination factors of drilled CFRP/titanium stacks using image processing and analysis techniques, and Marques et al. [30] successfully determined the delamination factors of holes in drilled composite and aluminium (CFRP/Al) multi-materials via computational analysis of X-ray images. Several non-destructive tests could acquire images of the hole and surrounding areas for the damage extension analysis and evaluation, such as radiogra-

phy, ultrasound, acoustic emission, C-scan, and computer tomography (CT) [24]. Despite this, the delamination damage was typically assessed using X-ray radiography, as it is the cheapest and most easily accessible imaging modality.

The problem is that the common software used to assess drilled multi-material hole damage had some gaps. For example, in many of them, the original hole images required manual pre-editing to obtain consistent results, which were sometimes incorrect, nonetheless. They also required several user inputs of key functions that, if wrongly selected, led to problems in their functioning. Additionally, the main limitation of solutions developed in Matlab is that it is a paid software, whereas those developed in Python have no such limitation and can be improved easily with new functions associated with the Python libraries that appear every day. Therefore, the objective of this work consisted in the development of an algorithm in Python with an intuitive interface, i.e., an enhanced graphical user interface (GUI), which uses image processing and analysis techniques to obtain comprehensive information about the quality of drilled holes in CFRP/Al multi-material, namely the extent of delamination, from X-ray images. The algorithm was then compared to a previous algorithm developed in Matlab to confirm its superior performance, mainly in terms of image improvement and accuracy of delamination factors. For this, it was necessary to perform the division of the problem under study into two main steps:

- Image processing, where the input image was firstly improved by enhancing its most relevant features and via contrast refinement and noise smoothing to retain only the regions of interest with enhanced quality.
- Image segmentation and analysis, where the region of interest was selected through proper thresholding and finally assessed, resulting in the evaluation of the hole's damage based on delamination factors derived from its perimeter and area.

2. Materials and Methods

2.1. Image Acquisition

This work was based on a drilling campaign using a DMG Mori DMU 60 eVo (DMG Mori, Bielefeld, Germany) CNC machine on a three-layered multi-material (CFRP/Al/CFRP) with a 4.5 mm thickness, using a 6 mm diameter conventional twist drill with a point angle of 120° and helix angle of 30°. The multi-material was evenly distributed, with each layer having a thickness of 1.5 mm. The metal used was Al2024-T3, and the composite was a cross-ply (0/90°) with a thermosetting matrix (epoxy) composed of 7 plies.

For the acquisition of the intended images from the drilled holes, a radiography system associated with a Kodak RVG 5100 (Eastman Kodak Company, Rochester, NY, USA) digital sensor was used, Figure 2a, since the X-ray could effectively pass through both the CFRP and aluminium, revealing the damage present in them, as has been considered in several studies in the literature. Two foam supports were used on both sides of the sensor for the stacks' stability and to ensure that all the images were obtained with the same distances between the sensor and the plate and the sensor and the emissary. Firstly, the samples were immersed in a contrasting liquid, Analar Normapur Diiodomethane, for 30 min. Thus, when the X-ray system was employed, it revealed the zones where the liquid penetrated the delamination areas, which were clearly distinguished from the unaffected material because the liquid was opaque to radiography. As already mentioned, a Satelec X-mind radiography system was used, Figure 2b, with a 0.16 s exposition time, alongside the image acquisition software in Matlab and Python languages.

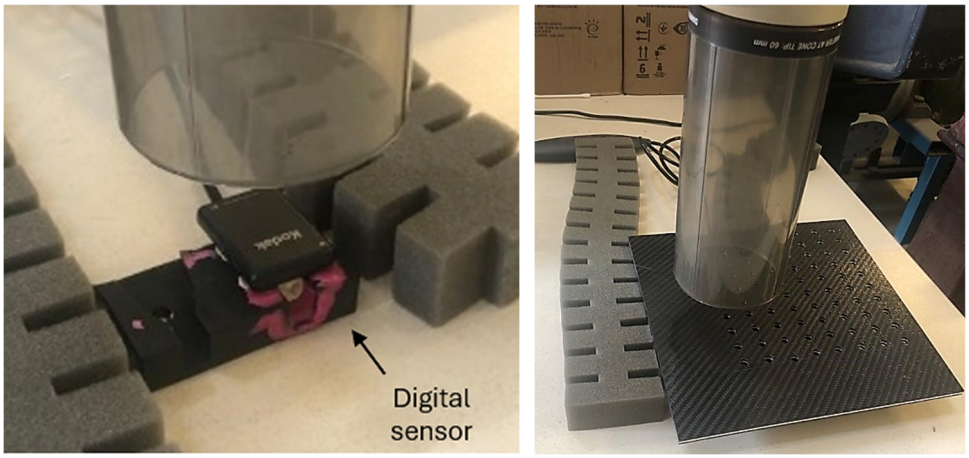

(**a**) (**b**)

Figure 2. (**a**) The Kodak RVG 5100 digital sensor and (**b**) a sample of the multi-material under X-ray analysis.

2.2. Algorithm Pipeline

Python was used to develop the image processing and analysis algorithm, mainly to identify the ROIs, i.e., the hole and damaged areas, and assess them. Its main steps consisted of image processing to determine the damaged and hole regions, image segmentation to determine the ROIs, and image analysis to calculate the delamination factors (Equations (1)–(3)). Finally, the results were shown to the user. The scheme in Figure 3 depicts the tasks performed in the novel algorithm. The development was based on the defined objectives and a literature search for Python functions that could be used to address the tasks involved. Combining different functions to obtain the desired outcome was possible with a trial-and-error method. The libraries in Python used to develop the new algorithm are shown in numpy v1.20.3, OpenCV v4.5.2, matplotlib v3.4.3 and scipy v1.7.3.

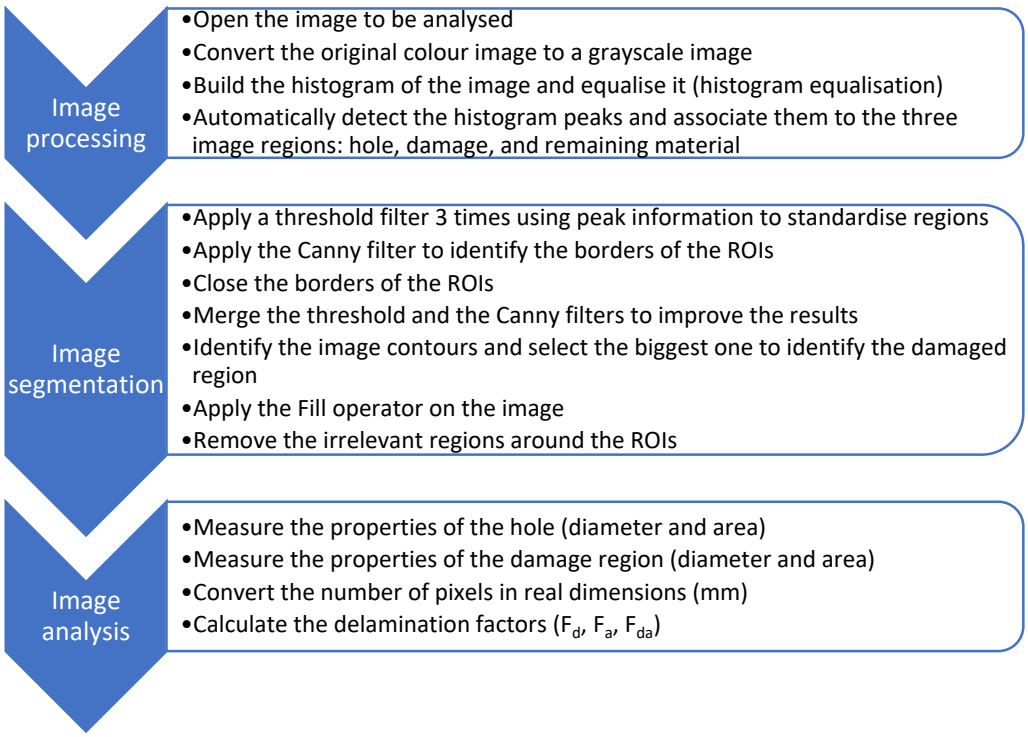

Figure 3. Pipeline of the novel image processing and analysis algorithm developed in Python.

3. Algorithm Comparison

3.1. Previous Algorithm

With the previous image processing and analysis algorithm developed in Matlab, when a new image is given as the algorithm's input, the first step is to manually choose the ROI's borders using a two-step selection grid, Figure 4, so that the algorithm may restrict the analysis to the specified region. From this selection and based on a conversion factor from pixels to millimetres (mm) that the user needs to update in the algorithm code before running it, the hole's radius is calculated first in pixels and then in mm.

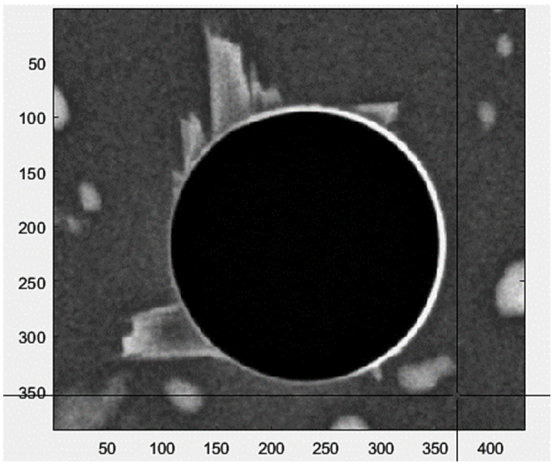

Figure 4. Grid selection of the ROI's borders of the hole image under study in the previous Matlab algorithm.

Afterward, the algorithm suggests a threshold that usually never corresponds to the intended one. It is either too high, as in Figure 5a, meaning that almost no delamination is detected and the hole circle is not entirely detected, or too low, as in Figure 5b, with unwanted noise surrounding the hole's region and disrupting the real delamination analysis. Therefore, the algorithm asks the user if the threshold is acceptable, and if the user declines it, the algorithm then asks the user to choose another value in an iterative method until a satisfying result is obtained, as in Figure 5c. Thus, an adequate threshold needs to be selected by the user based on visual analysis, otherwise, the delamination factors are miscalculated.

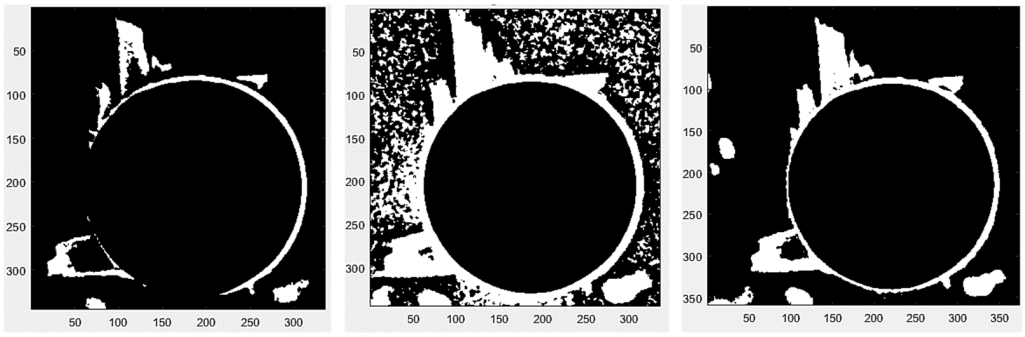

(**a**) (**b**) (**c**)

Figure 5. The effect of the selected ROIs threshold value in the previous Matlab algorithm: (**a**) too high, (**b**) too low, and (**c**) adequate threshold value.

Then, if the user accepts the threshold, it is necessary to zoom in on the image and press a random keyboard key. The problem is that the user can only determine that a pixel on the hole's border needs to be selected after pressing the key, and the user cannot zoom the image out at this step. Hence, an error occurs if a bad selection is made, and the process

must be reinitiated to continue. A similar process starts for the user to select a pixel on the delamination contour. Figure 6a and Figure 6b represent the hole and delamination contour detection, respectively, on the top left corner region of the image in Figure 5c.

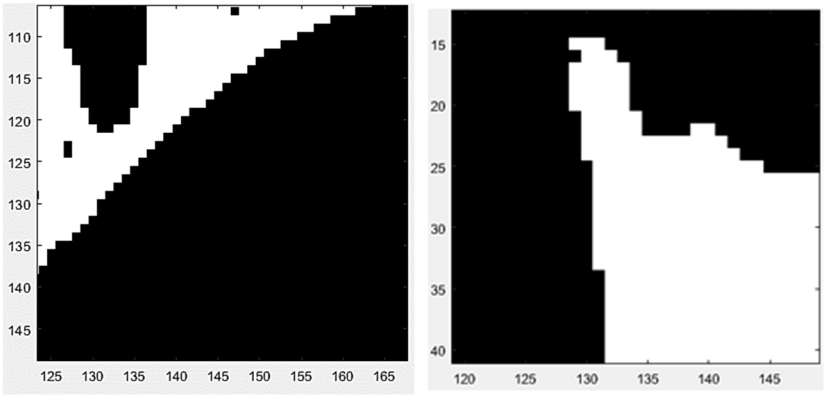

(**a**) (**b**)

Figure 6. Results obtained by the previous Matlab algorithm: the (**a**) hole and (**b**) delamination contour detection on the top left corner region of the image in Figure 5c.

At the final step of running the previous algorithm, it returns three images, one highlighting the hole region, Figure 7a, another representing the hole and damaged regions merged, Figure 7b, and finally, the binary image to be assessed, Figure 7c. Alongside these visual representations, the delamination factor values are presented to quantify the damage from the drill effect on the hole's periphery.

(**a**) (**b**) (**c**)

Figure 7. Results obtained by the previous Matlab algorithm: (**a**) the hole region, (**b**) the hole + damaged regions, and (**c**) the final binary image to be assessed.

3.2. Novel Algorithm

Considering the operational concerns mentioned earlier, a new algorithm needed to be developed, to enable easier operation and better result accuracy. Thus, a new set of steps was designed as follows:

- Image processing to determine the damaged and hole regions, i.e., image segmentation or determination of the ROIs.
- Calculating the delamination parameters: F_d, F_a, F_{da}.
- Showing the results to the user.

Figure 8 shows an example of a grayscale image imported to the new Python algorithm.

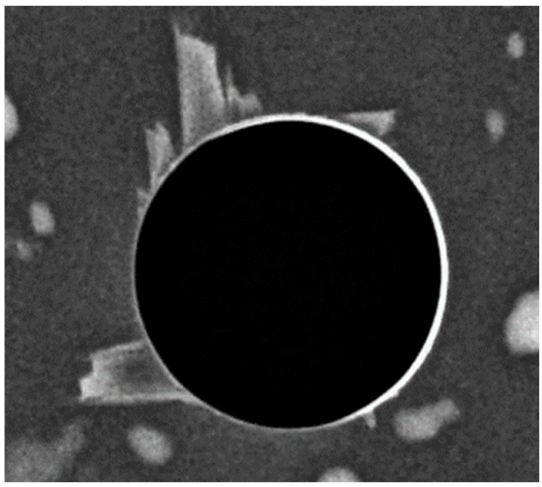

Figure 8. An example of a hole image imported to the new Python algorithm.

3.2.1. Image Segmentation—Determination of the ROI

The best way to analyse an image is to look at its histogram, like the one in Figure 9a. The histogram shows the number of pixels along each bright intensity. The original image essentially contained three groups of pixels, black, grey, and white, which could be analysed in the peaks of the respective histogram (Figure 9a) although the last one, with nearly 250 bins, was not very pronounced. To automatically determine the threshold indicated for each image, the value of each peak was calculated, Figure 9b, with only a small range given to define the values of that peak. The purpose of these two graphics was to show the approach used in the algorithm to identify the hole and damaged regions.

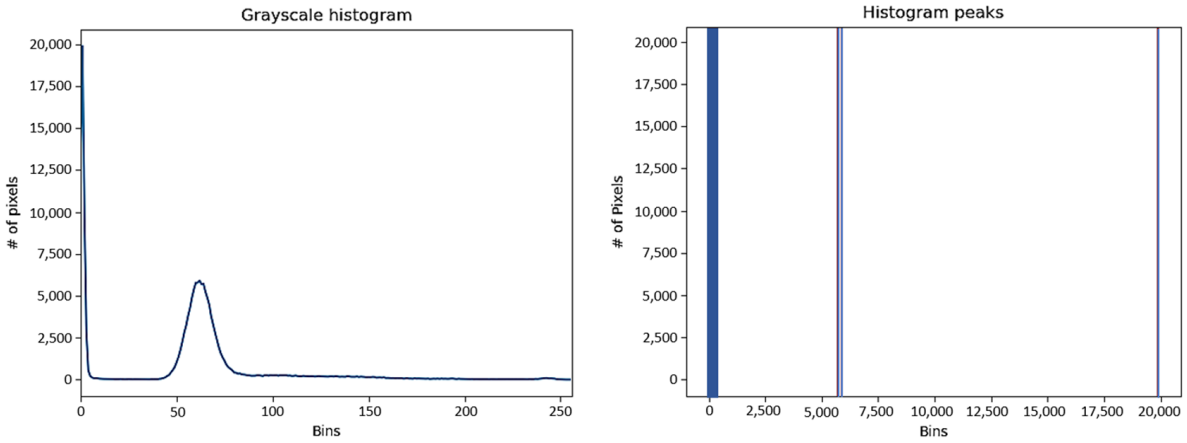

(**a**) (**b**)

Figure 9. (**a**) The grayscale histogram of the image in Figure 8 and (**b**) the respective histogram peaks.

The images in Figure 10 were obtained from the histogram data. Figure 10a,b resulted from the values of the peaks identified in Figure 9, showing the hole and damaged regions, respectively, by simply applying a threshold to those values given the respective interval. Figure 10c combines Figure 10a,b, showing the hole and damaged regions.

(**a**) (**b**) (**c**)

Figure 10. The output obtained by the new Python algorithm from the image in Figure 8: (**a**) the hole region, (**b**) the damaged region, and (**c**) the hole + damaged regions.

In the case of Figure 11, two different filters were applied to the original image. The Canny filter is commonly used to find objects' edges in images. This filter was tested, and examples of its results are shown in Figure 11a. Since this filter only shows the hole's edges, and there can be cases where the edges are not all closed, and there are gaps in the objects' borders, basic morphological filters were tested to improve the results. The combination of dilation and erosion operators after applying the Canny filter was the method that improved the results the most, Figure 11b.

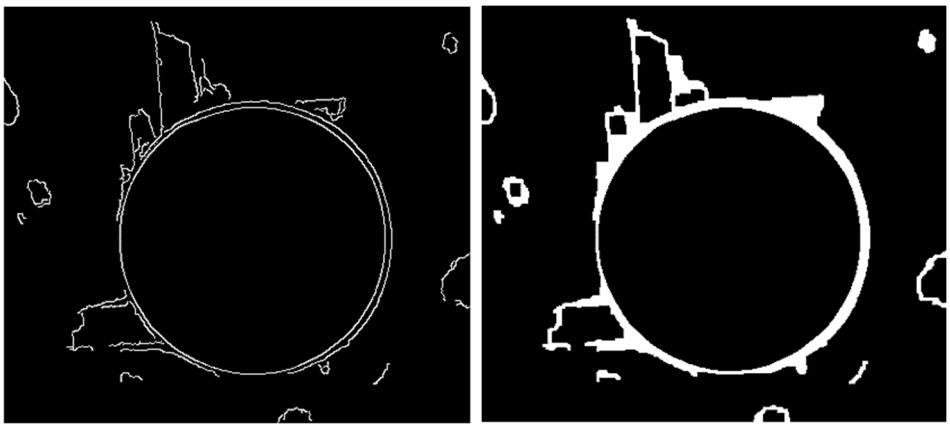

(**a**) (**b**)

Figure 11. Images after applying the (**a**) Canny edges detector and (**b**) erosion filter to the image in Figure 10c.

Figure 12a depicts the result of combining the previously applied filters with the threshold technique. Figure 12b shows the damaged and hole regions merged together, derived from Figure 12a by closing its borders, filling in the insides, and selecting only the region with the biggest area. At this step, the unwanted surrounding noise disappeared due to the combined action of the previously used filters. Figure 12c was obtained by replacing the central area (white pixels) of Figure 12b with the value of the hole region (black pixels), showing only the damaged region, so a proper comparison with the original image could be possible.

(**a**) (**b**) (**c**)

Figure 12. The output obtained by the new Python algorithm from the image in Figure 8: after the (**a**) filter combination, (**b**) filled damaged + hole region, and (**c**) damaged region.

3.2.2. Calculating the Delamination

This step calculates the delamination parameters by automatically counting the pixels corresponding to each region. Then, by knowing the base radius of the drilled hole, the conversion factor is calculated so that the delamination factors can be determined in mm. The X-ray images processed by the Python algorithm permitted a specific delamination evaluation to be quantified through delamination factor criteria (Equations (1)–(3)).

To determine the diameters for calculating the delamination factors, first, the contours of the hole and the damaged regions were identified by thin internal lines. Secondly, the smallest circle that included those contours was calculated on the thicker lines, corresponding to the hole's inner diameter, D_{nom}, Figure 13a, and the outer diameter of the circle better adjusted to the complete delaminated region, D_{max}, Figure 13b. In the first image, a slight difference between the two lines in the top left-hand corner is seen, which means that the hole was not perfectly circular, possibly caused by more loads being applied on that side during the drilling process.

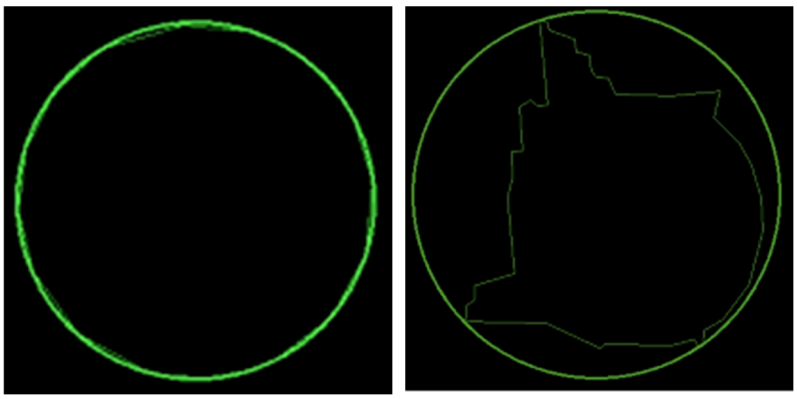

(**a**) (**b**)

Figure 13. The identification process of the (**a**) inner diameter, D_{nom}, and (**b**) delaminated outer diameter, D_{max}, by the new algorithm.

4. Novel Algorithm's Results

In order not to simply write the new algorithm's results in the user console, as the user may not be proficient in programming with Python or may use different code compilers, the results were presented under the image form for clearer output. For comparison purposes, the two algorithms were put side by side to highlight their differences, and the improvements brought by the new one in the analysis of two holes performed with different sets of parameters with distinct delamination levels.

Hole 1 was drilled with a feed of 0.3 mm/rev. and a cutting speed of 150 m/min. Comparing its original image, Figure 14a, with the corresponding binary image obtained

by the previously developed Matlab algorithm, Figure 14b, and the image obtained by the new Phyton algorithm, Figure 14c, a clear difference was observed. Particularly noticeable was the identification of the delaminated zones around the drilled hole, which in this new solution was highlighted more, with the delamination regions fully filled, contrary to the result obtained by the previous algorithm. Moreover, the presence of contrasting liquid drops near the hole, which could not be completely removed despite thoroughly cleaning the sample, leaving only the delaminated zones impregnated with it, can sometimes affect the damage assessment. The new algorithm successfully considered these as image noise and removed them so there was no interference with the delaminated region around the hole. This ensured a higher accuracy of the results, making the evaluation more precise and effective.

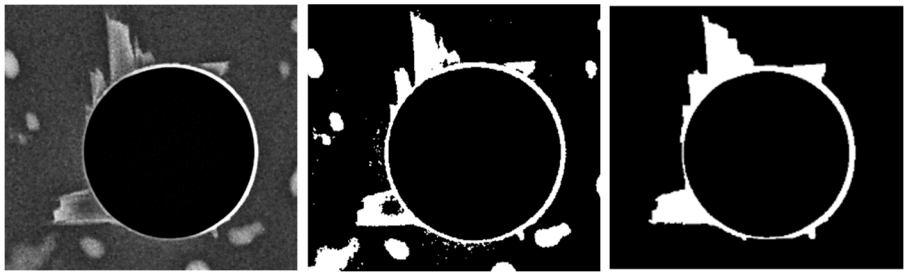

(**a**) (**b**) (**c**)

Figure 14. (**a**) The original image of Hole 1, (**b**) the output from the Matlab algorithm of the Hole 1 image, and (**c**) the corresponding output from the Python algorithm.

An example of a less damaged hole, namely of the Hole 2 image, drilled with a lower feed, 0.15 mm/rev., and the same cutting speed, 150 m/min., is depicted in Figure 15a. The problem with the previous algorithm, Figure 15b, was that if the selected threshold was too high, the hole's boundaries were not properly identified, but if it was too low, as shown in the image, there was too much noise around the hole. As clearly seen, the new algorithm, Figure 15c, was designed to identify better the less prominent delamination zones around the hole, i.e., the ones where the contrast liquid did not penetrate as effectively or were simply less deep and not so easily distinguishable with the naked eye. In the new algorithm, combining the Canny, dilation and erosion operators, and threshold filter removed the noise from the input image without compromising the hole boundaries, thus overcoming this problem.

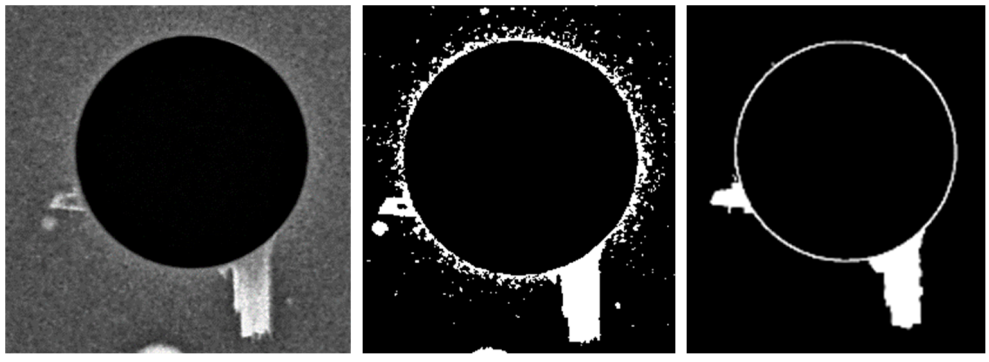

(**a**) (**b**) (**c**)

Figure 15. (**a**) The original image of Hole 2, (**b**) the output from the Matlab algorithm of the Hole 2 image, and (**c**) the corresponding output from the Python algorithm.

With the application of the new algorithm, obtaining more accurately adjusted delamination factors from images of holes with great delamination was possible. It also resulted in logical values regarding the tool used, and the chosen machining parameters, namely

the feed and cutting speed. Table 1 indicates the delamination factors calculated using Equations (1)–(3) with the data obtained from the images of Holes 1 and 2 by the previous and the new algorithms, along with the respective drilling parameters. Noticeably, the increase in the delamination factor obtained by the new algorithm was directly related to the feed increment.

Table 1. The comparison of the values of the studied delamination damage factors obtained from the images of Holes 1 and 2 using the two algorithms.

Hole Image	Feed (mm/rev)	Cutting Speed (m/min)	Algorithm	F_d	F_a	F_{da}
1	0.30	150	Previous	2.014	−0.239	1.380
			New	1.496	4.106	3.957
2	0.15	150	Previous	2.332	0.121	2.563
			New	1.366	3.492	3.383

The previous algorithm had problems with the image processing step and with calculating the delamination factors. Although the values of the adjusted delamination factor (F_{da}) seemed more reliable in the previous algorithm, as they were lower, it quickly became apparent that they were incorrect. The value in the Hole 2 image was almost twice as high as that in the Hole 1 image, and it can be perceived visually that the Hole 1 image contained more delamination than the second image. Using the new algorithm, the Hole 1 image had a higher adjusted delamination factor (F_{da}), but the two values were closer to each other, which is more realistic. Additionally, the delamination factor considering the area (F_a) obtained by the previous algorithm was too low, which does not make sense. Since it is calculated via the area, it should be higher than one, which only happens with the new algorithm.

All the calculated delamination factors are considerably above the acceptable limit in the aeronautical industry, which is 1.200 [31], which means that, as confirmed visually, the holes exhibit severe damage and would not be accepted in a quality inspection. Nevertheless, with the aid of the new Python algorithm, a correct analysis can be performed, ensuring better hole assessment and higher quality in obtaining good results in future experiments.

5. Discussion

The literature contemplates some works in this field, although the most common ones focus on drilling composites, such as CFRP. For example, Krishnaraj et al. [32] performed drilling tests in a 4.2-mm-thick unidirectional CFRP, obtaining an F_d of 1.33 with a feed of 0.2 mm/rev. and a cutting speed of 15 mm/min. In the work of Durão et al. [24], a 4-mm-thick unidirectional epoxy CFRP was drilled with feeds of 0.03, 0.1, and 0.2 mm/rev. and a constant cutting speed of 52 m/min, which resulted in F_d, F_{da} values of 1.29, 1.47, 1.61, 1.81, 2.04, and 2.33, respectively. In both studies, the F_d values were close to the multi-material ones, but in the second, the F_{da} values were relatively lower. Studies regarding the delamination quantification and analysis of drilling multi-materials, specifically CFRP/Al, are also being conducted, although not very prominently. Nevertheless, few articles can be found with the delamination values clearly stated and, from the existing ones, the majority only address the F_d factor, the simplest delamination factor. This is the case in Mahdi et al. [33], where they drilled into a 7.6-mm-thick woven CFRP/Al stack with an uncoated classical twist drill, obtaining F_d values of around 1.2 using a feed of 0.0023 mm/min. and a cutting speed of 178 m/min. Furthermore, Ekici et al. [34] drilled a 5-mm-thick woven CFRP/Al multi-material composed of seven alternate material layers with a twist drill containing a TiN–TiAlN PVD coating, achieving F_{da} results of 1.8 using a feed of 0.2 mm/rev. and a cutting speed of 85 m/min. This value is lower than the one obtained

in this present study, which means that the tool coating and stack configuration greatly influence the final hole quality when drilling multi-materials.

6. Conclusions

The main objective of this work was to develop an algorithm in Python that could solve the problems felt using an algorithm previously developed in Matlab in the correct processing and analysis of X-ray images of drilled holes in a multi-material, specifically, a CFRP/Al material. The established goals were reached with the new algorithm, in addition to the fact that it is free, meaning that it is available for any user to benefit from, in contrast to the previous one, which required paid software. With the implementation of the novel algorithm, it is now possible to select an image with the hole delamination as an input, and automatically identify the different zones without manual intervention. This avoids errors usually made by inexperienced users, such as selecting the wrong image threshold, which may lead to a failure and the need to start the procedure from the beginning, whereas in the Python algorithm, the threshold is defined automatically and, thus, is always the preferred option. Besides this, the developed algorithm correctly segments the input image into the hole, delamination, remaining material, and noise, giving more reliable results when calculating the delamination factors. To corroborate this, the quality of two drilled holes was assessed using both algorithms. Using the Matlab algorithm, the delamination factors obtained were equal to 1.380 and 2.563 for the two holes, respectively, while the results obtained using the Python algorithm were equal to 3.957 and 3.383, respectively. However, the first results were incorrect, as could easily be confirmed visually, the first hole had a higher delamination area, which was not suggested by the results obtained by the Matlab algorithm. In contrast, the results obtained by the Python algorithm were correct. In addition, the user of the new Python algorithm did not need any previous experience in image processing and analysis, and therefore, the analysis was quicker, and the results were more accurate. This algorithm can be applied to drilling images and any procedure involving delamination and fibre pull-out in composite materials. In the future, the new algorithm can be tested in other hole-making processes to quantify the damage around the hole, and possible improvements can be implemented to achieve results even more accurately for those processes.

Author Contributions: Conceptualization, R.D.F.S.C., M.L.S.B. and J.M.R.S.T.; methodology, R.D.F.S.C., F.G.A.S. and J.M.R.S.T.; software, R.D.F.S.C. and M.L.S.B.; validation, L.M.P.D.; formal analysis, T.E.F.S.; investigation, R.D.F.S.C. and M.L.S.B.; resources, T.E.F.S. and A.M.P.d.J.; data curation, R.D.F.S.C.; writing—original draft preparation, R.D.F.S.C.; writing—review and editing, T.E.F.S., F.G.A.S. and J.M.R.S.T.; visualization, M.L.S.B.; supervision, A.M.P.d.J. and F.J.G.S.; project administration, T.E.F.S. and A.M.P.d.J.; funding acquisition, T.E.F.S. All authors have read and agreed to the published version of the manuscript.

Funding: This research was funded by Project "Hi-rEV—Recuperação do Setor de Componentes Automóveis" (C644864375-00000002), cofinanced by "Plano de Recuperação e Resiliência" (PRR), "República Portuguesa", through NextGeneration EU program.

Data Availability Statement: The used data can be provided upon request.

Acknowledgments: The authors would like to thank Rui Silva and Miguel Figueiredo from DEMec-FEUP for supporting the X-ray analysis.

Conflicts of Interest: The authors declare no conflicts of interest.

References

1. Mohan, A.; Poobal, S. Crack detection using image processing: A critical review and analysis. *Alex. Eng. J.* **2018**, *57*, 787–798. [CrossRef]
2. Gonzalez, R.E.; Rafael, C. *Woods, Digital Image Processing*, 3rd ed.; Taylor & Francis: Upper Saddle River, NJ, USA, 2008.
3. Ahad, M.A.R.; Kobashi, S.; Tavares, J.M.R.S. Advancements of Image Processing and Vision in Healthcare. *J. Healthc. Eng.* **2018**, *2018*, 3–6. [CrossRef] [PubMed]

4. Gavaskar, R.G.; Chaudhury, K.N. Fast Adaptive Bilateral Filtering. *IEEE Trans. Image Process.* **2019**, *28*, 779–790. [CrossRef] [PubMed]
5. Yin, D.; Lopes, R.G.; Shlens, J.; Cubuk, E.D.; Gilmer, J. A fourier perspective on model robustness in computer vision. *Adv. Neural Inf. Process. Syst.* **2019**, *32*. [CrossRef]
6. Huang, S.; Yan, W.; Jean, S.; Mavromatis, S. Shallow-Water image enhancement using relative global histogram stretching based on adaptive parameter acquisition. *Multimed. Model.* **2018**, *71*, 453–465. [CrossRef]
7. Ulutas, G.; Ustubioglu, B. Underwater image enhancement using contrast limited adaptive histogram equalization and layered difference representation. *Multimed. Tools Appl.* **2021**, *80*, 15067–15091. [CrossRef]
8. Said, K.A.M.; Jambek, A.B. Analysis of Image Processing Using Morphological Erosion and Dilation. In *Journal of Physics: Conference Series*; IOP Publishing: Bristol, UK, 2021. [CrossRef]
9. Machado, J.M.; Tavares, J.M.R.S.; Camanho, P.P.; Correia, N. Automatic void content assessment of composite laminates using a machine-learning approach. *Compos. Struct.* **2022**, *288*, 115383. [CrossRef]
10. Zhang, Y.; Yuan, L.; Liang, W.; Member, S.; Zeng, Z. Carbon Fiber-Reinforced Polymer Composites Texture Angle Regression Based on the Improved Deep Hough Network. In *IEEE Journal of Emerging and Selected Topics in Industrial Electronics*; IEEE: Piscataway, NJ, USA, 2023; pp. 1–14. [CrossRef]
11. Cai, W.; Ma, Q.; Wang, Y.; Gan, X. Crashworthiness analysis and multi-objective optimization of Al/CFRP hybrid tube with initial damage under transverse impact. *Polym. Compos.* **2023**, *44*, 7953–7971. [CrossRef]
12. Wang, Z.; Wan, L.; Xiong, N.; Zhu, J.; Ciampa, F. Variational level set and fuzzy clustering for enhanced thermal image segmentation and damage assessment. *NDT E Int.* **2021**, *118*, 102396. [CrossRef]
13. Vinista, P.; Milton, M. A Novel Modified Sobel Algorithm for Better Edge Detection of Various Images. *Int. J. Emerg. Technol. Eng. Res.* **2019**, *7*, 25–31.
14. Barbosa, M.; Renna, F.; Dourado, N.; Costa, R. Construction of an Algorithm for Three-Dimensional Bone Segmentation from Images Obtained by Computational Tomography. *Stud. Comput. Intell.* **2023**, *1112*, 47–71. [CrossRef]
15. Feng, Q.; Gao, B.; Lu, P.; Woo, W.L.; Yang, Y.; Fan, Y.; Gu, L. Automatic seeded region growing for thermography debonding detection of CFRP. *NDT E Int.* **2018**, *99*, 36–49. [CrossRef]
16. De Albuquerque, V.H.C.; Silva, C.C.; de S, T.I.; Farias, J.P.; Tavares, J.M.R.S. Automatic evaluation of nickel alloy secondary phases from SEM images. *Microsc. Res. Tech.* **2011**, *74*, 36–46. [CrossRef] [PubMed]
17. Basivi, P.K.; Hamieh, T.; Kakani, V.; Pasupuleti, V.R.; Sasikala, G.; Heo, S.M.; Kim, C.W. Exploring advanced materials: Harnessing the synergy of inverse gas chromatography and artificial vision intelligence. In *TrAC-Trends in Analytical Chemistry 173*; Elsevier B.V.: Amsterdam, The Netherlands, 2024. [CrossRef]
18. Cruz, D.J.; Amaral, R.L.; Santos, A.D.; Tavares, J.M.R.S. Application of Digital Image Processing Techniques to Detect Through-Thickness Crack in Hole Expansion Test. *Metals* **2023**, *13*, 1197. [CrossRef]
19. Zhang, L.; Liu, Z.; Tian, W.; Liao, W. Experimental studies on the performance of different structure tools in drilling CFRP/Al alloy stacks. *Int. J. Adv. Manuf. Technol.* **2015**, *81*, 241–251. [CrossRef]
20. Blanco, D.; Rubio, E.M.; Marín, M.M.; Davim, J.P. Advanced materials and multi-materials applied in aeronautical and automotive fields: A systematic review approach. *Procedia CIRP* **2021**, *99*, 196–201. [CrossRef]
21. Chen, W.C. Some experimental investigations in the drilling of carbon fiber-reinforced plastic (CFRP) composite laminates. *Int. J. Mach. Tools Manuf.* **1997**, *37*, 1097–1108. [CrossRef]
22. Mohan, N.S.; Kulkarni, S.M.; Ramachandra, A. Delamination analysis in drilling process of glass fiber reinforced plastic (GFRP) composite materials. *J. Mater. Process. Technol.* **2007**, *186*, 265–271. [CrossRef]
23. Davim, J.P.; Rubio, J.C.; Abrao, A.M. A novel approach based on digital image analysis to evaluate the delamination factor after drilling composite laminates. *Compos. Sci. Technol.* **2007**, *67*, 1939–1945. [CrossRef]
24. Durão, L.M.P.; Tavares, J.M.R.S.; de Albuquerque, V.H.C.; Gonçalves, D.J.S. Damage evaluation of drilled carbon/epoxy laminates based on area assessment methods. *Compos. Struct.* **2013**, *96*, 576–583. [CrossRef]
25. Silva, J.M.; Ferreira, F.; Abreu, S.M.; Matos, J.E.; Durão, L.M.P. Correlation of drilling damage with mechanical strength: A geometrical approach. *Compos. Struct.* **2017**, *181*, 306–314. [CrossRef]
26. Devesa, L.F.S.; Matos, J.E.; Durão, L.M.P. Composites Part C: Open Access Experimental assessment of delamination extension on carbon/epoxy drilled plates. *Compos. Part C Open Access* **2021**, *5*, 100144. [CrossRef]
27. Geier, N.; Póka, G.; Jacsó, Á.; Pereszlai, C. A method to predict drilling-induced burr occurrence in chopped carbon fibre reinforced polymer (CFRP) composites based on digital image processing. *Compos. Part B Eng.* **2022**, *242*, 110054. [CrossRef]
28. Hernandez, A.; Maghami, A.; Khoshdarregi, M. A Machine Vision Framework for Autonomous Inspection of Drilled Holes in CFRP Panels. In Proceedings of the 2020 6th International Conference on Control, Automation and Robotics (ICCAR), Singapore, 20–23 April 2020; Volume 2020, pp. 669–675. [CrossRef]
29. Isbilir, O.; Ghassemieh, E. Comparative study of tool life and hole quality in drilling of CFRP/titanium stack using coated carbide drill. *Mach. Sci. Technol.* **2013**, *17*, 380–409. [CrossRef]
30. Marques, F.; Silva, F.G.A.; Silva, T.E.F.; Rosa, P.A.R.; Marques, A.T.; de Jesus, A.M.P. Delamination of Fibre Metal Laminates Due to Drilling: Experimental Study and Fracture Mechanics-Based Modelling. *Metals* **2022**, *12*, 1262. [CrossRef]

31. Ahmad Sobri, S.; Whitehead, D.; Mohamed, M.; Mohamed, J.J.; Mohamad Amini, M.H.; Hermawan, A.; Norizan, M.N. Augmentation of the delamination factor in drilling of carbon fibre-reinforced polymer composites (CFRP). *Polymers* **2020**, *12*, 2461. [CrossRef]
32. Krishnaraj, V.; Zitoune, R.; Collombet, F.; Davim, J.P. Challenges in drilling of multi-materials. *Mater. Sci. Forum* **2013**, *763*, 145–168. [CrossRef]
33. Mahdi, A.; Turki, Y.; Habak, M.; Salem, M.; Bouaziz, Z. Experimental study of thrust force and surface quality when drilling hybrid stacks. *Int. J. Adv. Manuf. Technol.* **2020**, *107*, 3981–3994. [CrossRef]
34. Ekici, E.; Motorcu, A.R.; Yıldırım, E. An Experimental Study on Hole Quality and Different Delamination Approaches in the Drilling of CARALL, a New FML Composite. *FME Trans.* **2021**, *49*, 950–961. [CrossRef]

Disclaimer/Publisher's Note: The statements, opinions and data contained in all publications are solely those of the individual author(s) and contributor(s) and not of MDPI and/or the editor(s). MDPI and/or the editor(s) disclaim responsibility for any injury to people or property resulting from any ideas, methods, instructions or products referred to in the content.